

THE INTERNATIONAL JOURNAL OF SCIENCE & TECHNOLEDGE

Physical Properties and Structural Analysis of Activated Carbon Produced from *Canarium Schweinfurthii* Seed Using Acetic Acid as Alternative Reagent and Its Application on Dye Effluent

Moshood Olayinka Ahmed

Regulatory Officer, Department of Chemistry,
Abubakar Tafawa Balewa University Bauchi, Nigeria

Dr. Boryo D.E.A.

Senior Lecturer, Department of Chemistry,
Abubakar Tafawa Balewa University Bauchi, Nigeria

Dr. Mahmoud A.A.

Senior Lecturer, Department of Chemistry,
Abubakar Tafawa Balewa University Bauchi, Nigeria

Abstract:

Activated carbon was produced from *Canarium schweinfurthii* seed by physical and chemical processes. Acetic acid was used as alternative chemical at various concentrations (30 – 60%). The reaction conditions were optimized at temperature range 400 – 600 °C and time interval of 20 – 60 minutes. The raw atile seed and carbonized charcoal were characterized using parameters like bulk density, percentage yield, moisture content, ash content and percentage of carbon. The uncarbonized atile seed has a bulk density of 0.4348, percentage yield 93 %, moisture content 4.7 %, ash content 2.3 % and percentage of carbon 93 %, while the carbonized charcoal at temperature range of (400 – 600 °C) has a bulk density of (0.4115 – 0.4312 g/cm³), percentage yield (80.82 – 86.48 %), moisture content (13 – 17 %), ash content (6 – 2 %) and percentage of carbon of (74.005 – 84.510 %). The activated carbon was further used to decolourize dye effluent. The experimental data were analyzed using Langmuir, Freundlich and Dubinin-Radushkevich isotherms. After optimization, the activated carbon was structurally analyzed using Fourier-transform infrared spectroscopy (FTIR), Scanning electron microscope (SEM), Brunauer-Emmett-Teller (BET) and X-ray diffraction (XRD).

Keywords: Carbon, Domestic waste, Carbonization, Activation, Charcoal, Characterization.

1. Introduction

Activated carbon, also known as activated charcoal or activated coal is a form of carbon that has been processed to make it extremely porous, thereby making it to have large surface area which can then be used for chemical reactions and adsorption [1]. Over the years, use of activated carbon has evolved from medieval time to this modern day. Charcoal has been a household name many centuries ago and thus its importance and usefulness cannot be overemphasized [1]. As a result of its importance in all life's endeavors, this has led to searching for various agricultural byproducts to produce activated carbon.

Most domestic and agricultural byproducts are biodegradable, but some of them take time before being degraded completely, hence constituting environmental nuisance. El-Sayed et al. [2] said the production of activated carbon from agricultural byproducts has both economic and environmental effects, as it converts unwanted, low-value agricultural waste to useful high value adsorbent. Agricultural waste products like shell, husks, seeds, pods, stems, weeds are good sources of activated carbon production. Researchers have done extensive work on some agricultural byproducts like coconut shell, groundnut shell, and corn pods [2].

The aim of the research work is to determine the physical properties and structural analysis of activated carbon produced from domestic wastes namely *Canarium schweinfurthii* seed with acetic acid as alternative reagent.

2. Materials and methods

2.1. Experimental Section

Canarium schweinfurthii (Atile) seed was sourced from the University roundabout near University of Jos hostel, Jos, Plateau State Nigeria. 50 grams of pulverized *Canarium schweinfurthii* seeds were placed in jars containing 100 mls of three different reagents with impregnation ratio of 1:2, (IR 1:2). The jars were labelled appropriately as 30, 40 and 60 %

acetic acid. After 24 hours, the *Canarium schweinfurthii* seed solution was decanted leaving behind a sludge. The sludge of *Canarium schweinfurthii* seeds were packed into crucibles and placed in furnace. The reagents concentration was ranged from 30% to 60%, temperature of activation ranges from 400 °C to 600 °C as well as time of activation as varied at 20 minutes interval from 20 to 60 minutes

2.2. Proximate Analysis

Determination of Moisture content

1g of the sample was weighed and heated in watch glass at 105°C for 2 hours. Heated crucible was cooled and re-weighed [3].

$$\text{Moisture percentage} = (\text{Loss in weight on drying (g)})/(\text{Initial weight (g)}) \times 100 \quad (1)$$

Determination of Ash Content

3g sample was weighed and heated in open crucibles at 750°C for 1.5 hours. The crucible was then cooled and re-weighed [3].

$$\text{Ash percentage} = (\text{Ash weight})/(\text{Oven dry weight}) \times 100 \quad (2)$$

Determination of percentage yield of carbonized charcoal

Samples of bio-waste were dried and weighed and carbonized in a furnace at 400 °C, 500 °C and 600 °C for 1 hour. The charcoal product was weighed [4].

The percentage yield was calculated as follows:

$$\begin{aligned} \text{percentage yield} \\ &= (\text{weight of raw material} \\ &- \text{weight of carbonized raw material})/(\text{weight of raw material}) \times 100 \quad (3) \end{aligned}$$

2.2.1. Determination of Percentage of Carbon

Percentage of carbon in the raw material is determined by removing the Ash percentage and Moisture percentage from 100%.

$$\text{percentage carbon} = 100 - \text{Percentage ash} - \text{Percentage moisture} \quad (4)$$

2.2.2. Determination of Bulk Density

A small quantity of charcoal carbonized at 400 °C, 500 °C and 600 °C were taken and ground to powder; sieved and separately put into the density bottle and weighed. The weight and the volume of the density bottle had been initially determined. The bulk density was calculated using the following expression:

$$\text{Bulk density} = (\text{mass of carbon sample})/(\text{volume}) \quad (5)$$

2.2.3. Determination of Percentage Decolourization

Percentage decolourization was calculated using the following mathematical expression for each set of activated carbon and their effect on dye effluent:

$$\text{percentage} = (D_0 - D_1)/D_0 \times 100 \quad (6)$$

Where D_0 = initial dye effluent absorbance

And D_1 = Final dye effluent absorbance after application of activated carbon overnight

2.3. Adsorption Isotherms

Freundlich, Langmuir and Dubinin-Radushkevich isotherms were used to study the type of interaction between the prepared activated carbons and the dye effluent.

2.3.1. Freundlich Isotherm

This isotherm is an empirical equation and can be employed to describe heterogeneous systems.

$$\text{Where: } q_e = K_f C_e^{1/n} \quad (7)$$

Where q_e is the amount of substance adsorbed at equilibrium in (mg/g), C_e is the equilibrium adsorbate concentration in the fluid (mg/L), $1/n$ is a heterogeneity factor less than 1 if the adsorption process is favorable, K_f is the Freundlich constant which is a measure of adsorption capacity (mg/g). K_f can also be defined as the adsorption or distribution coefficient and represents the quantity adsorbed for a unit equilibrium concentration [5]. The linearized form of Freundlich model is given by the equation 2:

$$\log q_e = \log K_f + 1/n \log C_e \quad (8)$$

A plot of $\log q_e$ against $\log C_e$ gives a straight line with $1/n$ as slope and $\log K_f$ as intercept.

2.3.2. Langmuir Isotherm

The Langmuir isotherm assumes monolayer adsorption on a uniform surface with a finite number of adsorption sites. Once a site is filled, no further sorption can take place at that site. As such, the surface will eventually reach a saturation point where maximum adsorption at the surface is achieved [6]. The linear form of Langmuir isotherm model given by the equation 4 and the separation factor by equation 3:

$$C_e/q_e = 1/(K_L q_{max}) + 1/(q_{max} C_e) \quad (9)$$

$$RL = 1/(1 + K_L C_0) \quad (10)$$

Where C_e is the equilibrium concentration of the adsorbate (mg/L), q_e the amount adsorbed per unit mass of adsorbent (mg/g), K_L is the Langmuir adsorption constant and q_{max} is the maximum adsorption capacity (mg /g). R_L is a dimensionless constant referred to as separation factor or equilibrium parameter. If $R_L > 1$, the adsorption is unfavourable, $R_L = 1$ it is linear, $0 < R_L < 1$ the adsorption is favorable and if $R_L = 0$, the adsorption is irreversible.

2.3.3. Dubinin-Radushkevich Isotherm

The Dubinin-Radushkevich (D-R) isotherm is an empirical equation where the adsorption is characterized by multi-layer condensation involving van der Waals forces and is suitable for physisorption [7]. The expression for the linear form of the D-R isotherm is given by equation 5:

$$\ln q_e = \ln q_d - \beta \varepsilon^2 \quad (11)$$

Where q_d is the D-R constant which refers to maximum adsorption capacity β (mg/g), $(\text{mol}^2/\text{J}^2)$ is a constant related to free energy and ε is the Polanyi potential which is defined in equation 6 as:

$$\varepsilon = RT \ln [1 + 1/C_e] \quad (12)$$

Where R is the general gas constant ($8.314 \text{ J mol}^{-1} \text{ K}^{-1}$) and T is the absolute temperature. The constant β gives the mean free energy E (equation 7):

$$E = 1/\sqrt{2\beta} \quad (13)$$

If E values between 1–16 kJ/mol, this indicates physical adsorption while values above 16 kJ/mol indicate chemisorption [8].

3. Results and Discussions

Table 1 shows the physical properties of the raw material and the produced adsorbents. The lower ash content reveals that it is a useful candidate for adsorption. This assertion is agreed to by [9].

Physical Properties	Temperature (°C)	Uncarbonized atile
Bulk density (g/cm ³)		0.4348
Moisture content (Wt. %)		4.7
Ash content (Wt. %)		2.3
Percentage of Carbon (Wt. %)		93
Percentage yield (Wt. %)	400	86.48
	500	81.30
	600	80.82

Table 1: Physical Properties of the Uncarbonized Canarium Schweinfurthii Seed

Physical Properties	Temperature (°C)	Carbonized Atile
Bulk density (g/cm ³)	400	0.4115
	500	0.4299
	600	0.4312
Moisture content (Wt. %)	400	19.945
	500	15.907
	600	13.49
Ash content (Wt. %)	400	6
	500	2
	600	2
Percentage of Carbon (Wt. %)	400	74.055
	500	82.093
	600	84.510

Table 2: Physical Properties of the Carbonized Charcoal

The bulk density of the raw material is 0.4348 g/cm³, ash content 2.3%, moisture content 4.3%, carbon content 93% and percentage yields of the charcoal are 80.82%, 81.3%, and 86.48 at 400 °C, 500 °C and 600 °C respectively.

3.1. Effect of Carbonization on Bulk Density

The bulk densities as indicated in Table 1 and 2 above showed no significant difference as would have been expected. However, the bulk density of the raw atile in Table 1 was 0.4348 g/cm³ which is higher than the carbonized atile in Table 2. This observation supports the claim of Ekebafe *et al.* [10], which states that, at high heating temperature, the bulk density reduces which may be due to the opening of the interstitial spaces (microspores) in the carbon residue.

3.2. Effect of Carbonization Ash Content

From the Table the determine ash contents is 2.3 % for the raw material. While after carbonization the ash content was determined as 6 % at 400 °C, 2 % at 500 °C and 2 % at 600 °C. The charcoal's ash content varies from 0.5 % to more than 5 % depending on raw materials. Good quality charcoal typically has the ash content of around 3 %, [11].

3.3 Effect of carbonization moisture content

The moisture content of the raw material is 4.7 %, however that of the carbonized materials ranged from 13 – 29 %. The high moisture content of carbonized raw material could be as a result adsorption of moisture. When charcoal is freshly prepared, the moisture content is around 1%. However, when charcoal is left overtime, the hygroscopicity is increased, hence moisture content of charcoal can rise up to 15 % or even more [11].

3.4. Effect of Carbonization on Percentage Yield

The percentage yield as seen in table 1 above indicated reduction in yield with increase in temperature from 86.48 at 400 °C to 80.82 at 600 °C. The rate of weight loss is primarily due to the initial large amount of volatiles that can be easily released with increasing temperature as well as the loss of moisture to a lesser extent [12].

3.5. Effect of carbonization on percentage of carbon

From the Table above (Table 1), the percentage of carbon increases with increasing temperature simply because the ash, moisture and volatile contents has reduced at that high temperatures. This observation is supported by Harry [11], and according to Ukrainian biofuel suppliers, the fixed carbon content of charcoal ranges from a low of about 50% to a high or around 95%.

S/N	Activated Carbon	pH
1	A9	5.1
2	B9	6.4
3	C9	6.6
4	D9	5.9
5	E9	5.1
6	F4	5.8
7	G7	4.1
8	H6	5.0
9	I9	6.2
10	J2	5.7
11	K2	5.4
12	L5	7.2

Table 3: Ph of the Optimized Activated Carbons

The pH of the raw material recorded at room temperature was 5.5, while the pH of the activated carbons as observed were highlighted in Table 3 above. And from the table the pH range is 4.1 to 7.2, clearly indicates that the range is Neutral.

3.6. Percentage Decolourization

The calculated percentage decolourization of the optimized samples are illustrated in Fig 1 below.

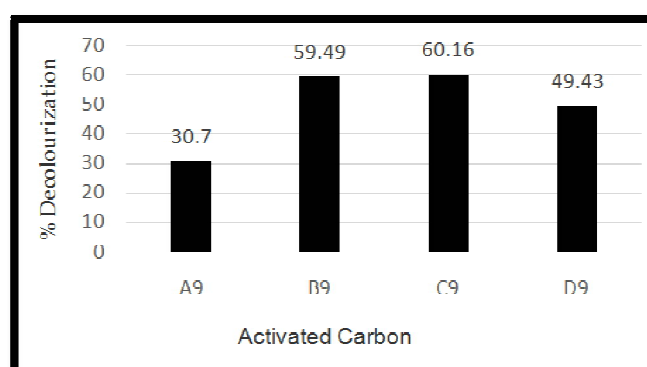


Figure 1: Optimum Conditions of Activated Carbon for Percentage Decolourization

Key 1:

A9----- 30% acetic acid activated carbon at 600°C for 60 minutes

B9-----40% acetic acid activated carbon at 600°C for 60 minutes

C9-----50% acetic acid activated carbon at 600°C for 60 minutes

D9-----60% acetic acid activated carbon at 600°C for 60 minutes

3.7. Surface Morphology

The micrograph of prepared activated carbons was presented in figure (2 - 5) respectively. These figures showed cavities, pores and rough surfaces. The surfaces are pitted and fragmented due to carbonization and activation using chemical method [9].

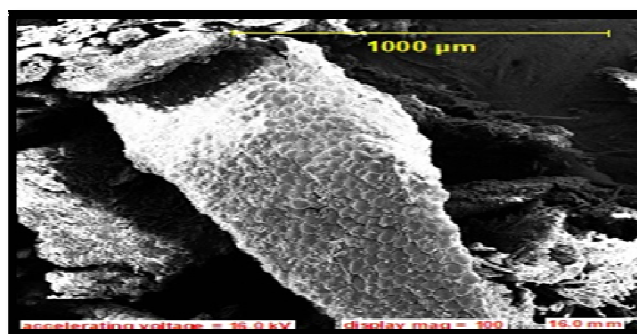


Figure 2: SEM Micrograph of Raw Canarium Schweinfurthii (Mag = 100)

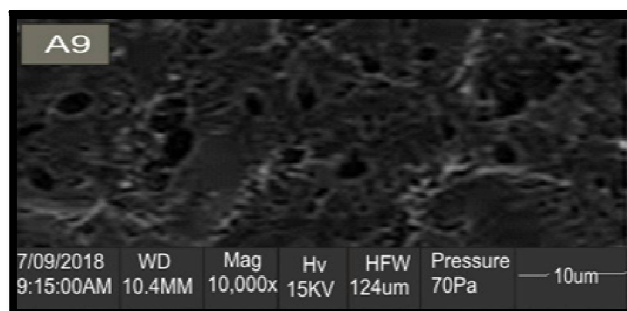


Figure 3: SEM Micrograph of Activated Carbon A9 (Mag = 10,000)

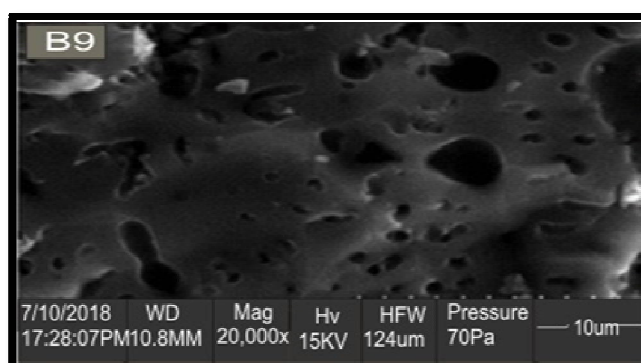


Figure 4: SEM Micrograph of Activated Carbon B9 (Mag = 20,000)

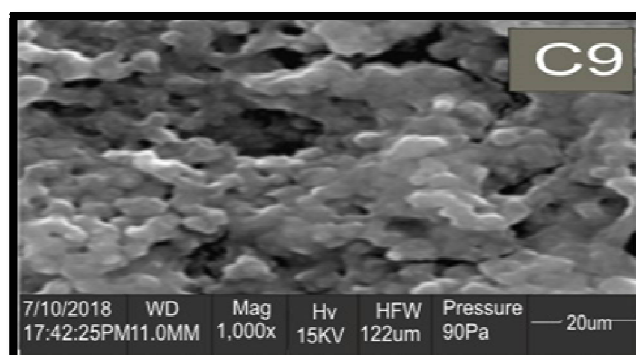


Figure 5: SEM Micrograph Of Activated Carbon C9 (Mag = 1000)

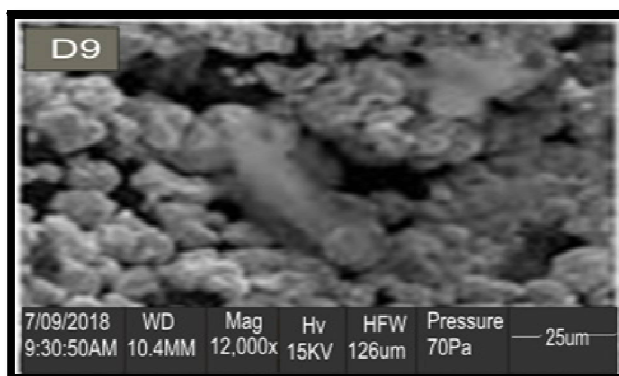


Figure 6: SEM Micrograph of Activated Carbon D9 (mag = 12,000)

3.7.1. Surface Area and Pore Characteristics

A9 (Fig1) showed some narrow pores on its surface which are formed when the precursor materials are subjected to heat treatment at the appropriate temperature and conditions [13] and [14].

B9 and C9 showed small dark spaces in its micrograph indicating the spores for adsorption. D9 showed small dark spaces in its micrograph indicating the spores for adsorption

A9		B9	
Temperature (T/°C)	Specific Surface Area (m ² /g)	Temperature (T/°C)	Specific Surface Area (m ² /g)
100	920.70	100	1068.80
200	943.61	200	1003.21
300	954.10	300	1300.45
400	940.00	400	998.56
500	943.60	500	1021.20
600	943.12	600	1052.30
Mean	940.86		1074.09

Table 4: Physical Properties of Carbonized Atile (A9 and B9) Using Brunauer-Emmett-Teller (BET)

C9		D9	
Temperature (T/°C)	Specific Surface Area (m ² /g)	Temperature (T/°C)	Specific Surface Area (m ² /g)
100	1060.80	100	657.30
200	1055.27	200	670.50
300	1300.45	300	690.20
400	1098.56	400	674.60
500	1027.20	500	676.20
600	1050.80	600	675.70
Mean	1098.85		674.08

Table 5: Physical Properties of Carbonized Atile (C9 and D9) Using Brunauer-Emmett-Teller (BET)

3.8. Effect of Carbonization on Canarium Schweinfurthii Using Brunauer-Emmett-Teller (BET)

A9 activated carbon has an average surface area of 940.86 m²/g, B9 is 1074.09 m²/g, and C9 has mean surface area of 1098.85 m²/g. however D9 has a lower average surface area of 674.08 m²/g. A9 and D9 are mesopores, while B9 and C9 are macropores,

3.9. Functional Groups

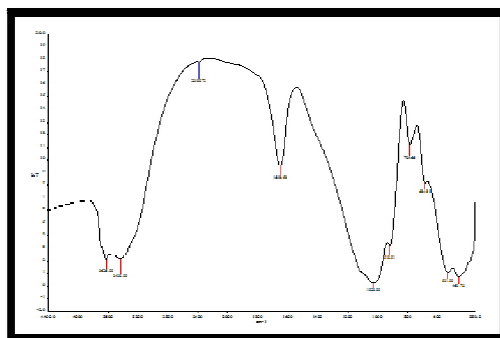


Figure 7: FTIR Spectra of A9

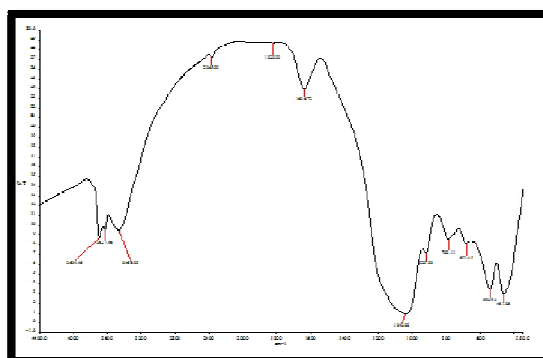


Figure 8: FTIR Spectra of B9

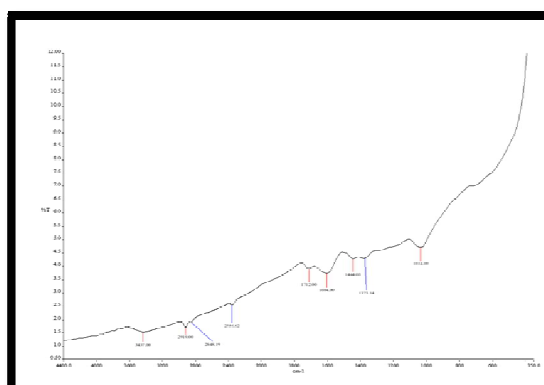


Figure 9: FTIR Spectra Of C9

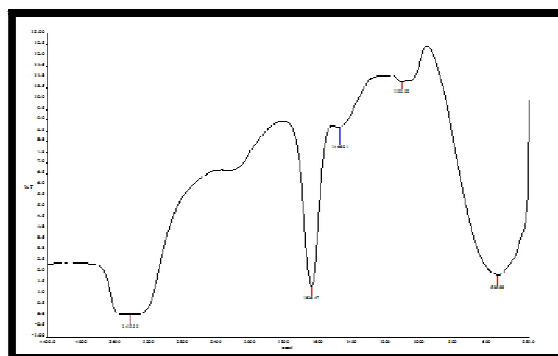


Figure 10: FTIR Spectra of D9

Infrared spectroscopy provides information on the chemical structure of the carbon material. Fig. (14-17) shows FTIR spectra of the synthetic carbons obtained by acetic acid activation at different concentrations (A9- D9). All spectra show a wide transmittance band ranging from 3419 - 3694 cm^{-1} . Spectra (3438.00, 3466.00, 3437.00 and 3419.00 cm^{-1}) can be assigned to the O-H stretching mode of hydroxyl groups and adsorbed water. The position and asymmetry of this band at lower wave numbers indicate the presence of strong hydrogen bonds (from carboxyls, phenols or alcohols) [15]. A weak sharp transmittance bands: $\sim 3600 \text{ cm}^{-1}$ were present in spectra of A9 and B9 activated carbons. This peak may be ascribed to isolated O-H groups.

The 2380.72 and 2365.00 cm^{-1} observed at A9 and B9, may be due to carbonates compounds during handling [16].

The FTIR spectrum of activated carbon B9 shows absorption bands due to saturated aliphatic bands Sp3 (2919.00 and 2848.19: C–H stretching in –CH). Also observed are small bands at about 1648.53 (A9), 1636.72 (B9), 1712.00 (C9) and 1636.47 cm⁻¹ (D9). These are usually assigned to C=O stretching vibrations of amide, ketones and carboxylic acids [16]. The band at 1028.00 cm⁻¹ for A9, 1042.00 cm⁻¹ for B9, 1034.00 cm⁻¹ for C9 and 1103.00 cm⁻¹ for D9 can all be assigned to C–O stretching mode [16]. This can therefore be attributed to existence of oxygenated functional group at the adsorbent surface [16], [17], [18].

Lastly, a C–C band is observed in C9 at 1444.00 cm⁻¹ (methylene group CH₂) and 1373.14 cm⁻¹ (methyl group CH₃). [16].

3.10. Adsorption Isotherms

Freundlich, Langmuir and Dubinin-Radushkevich isotherms were used to study the type of interaction between the prepared activated carbons and the dye effluent. Based on the values of experimental data using Langmuir, Freundlich and Dubinin-Radushkevich isotherms. The data best fitted to Freundlich and Langmuir Isotherm and less into D-R isotherm.

3.10.1. Freundlich Isotherm

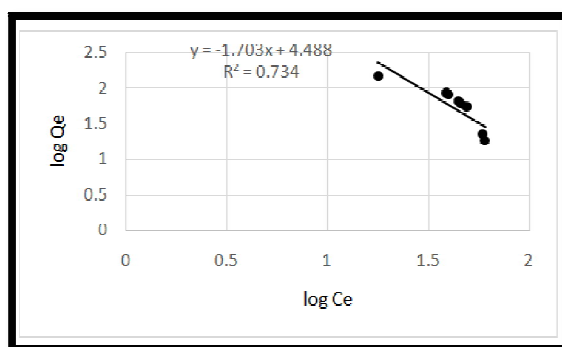


Figure 11: Freundlich Isotherm of A1-A9

Key 1:

- A1---30% acetic acid activated carbon at 400°C for 20 minutes
- A2---30% acetic acid activated carbon at 400°C for 40 minutes
- A3---30% acetic acid activated carbon at 400°C for 60 minutes
- A4---30% acetic acid activated carbon at 500°C for 20 minutes
- A5---30% acetic acid activated carbon at 500°C for 40 minutes
- A6---30% acetic acid activated carbon at 500°C for 60 minutes
- A7---30% acetic acid activated carbon at 600°C for 20 minutes
- A8---30% acetic acid activated carbon at 600°C for 40 minutes
- A9---30% acetic acid activated carbon at 600°C for 60 minutes

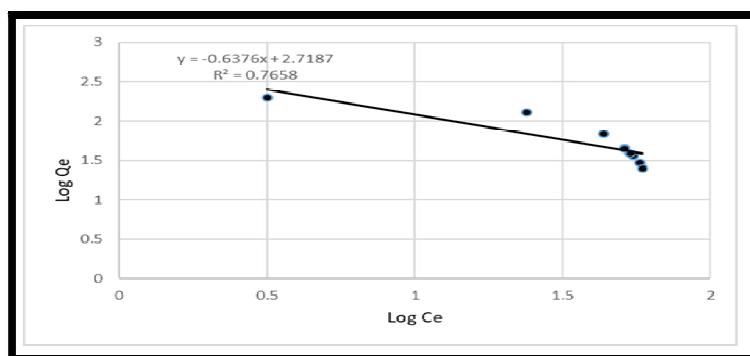


Figure 12: Freundlich Isotherm of B1-B9

- Key 2:
- B1--- 40% acetic acid activated carbon at 400°C for 20 minutes
 - B2--- 40% acetic acid activated carbon at 400°C for 40 minutes
 - B3--- 40% acetic acid activated carbon at 400°C for 60 minutes
 - B4--- 40% acetic acid activated carbon at 500°C for 20 minutes
 - B5--- 40% acetic acid activated carbon at 500°C for 40 minutes
 - B6--- 40% acetic acid activated carbon at 500°C for 60 minutes
 - B7--- 40% acetic acid activated carbon at 600°C for 20 minutes
 - B8--- 40% acetic acid activated carbon at 600°C for 40 minutes
 - B9--- 40% acetic acid activated carbon at 600°C for 60 minutes

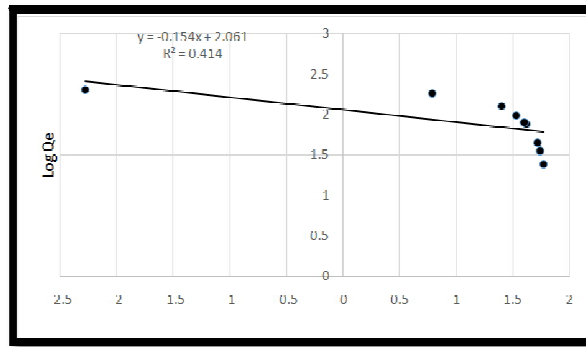


Figure 13: Freundlich Isotherm of C1-C9

Key 3: C1----- 50% acetic acid activated carbon at 400^oc for 20 minutes
 C2-----50% acetic acid activated carbon at 400^oc for 40 minutes
 C3-----50% acetic acid activated carbon at 400^oc for 60 minutes
 C4-----50% acetic acid activated carbon at 500^oc for 20 minutes
 C5-----50% acetic acid activated carbon at 500^oc for 40 minutes
 C6-----50% acetic acid activated carbon at 500^oc for 60 minutes
 C7-----50% acetic acid activated carbon at 600^oc for 20 minutes
 C8-----50% acetic acid activated carbon at 600^oc for 40 minutes
 C9-----50% acetic acid activated carbon at 600^oc for 60 minutes

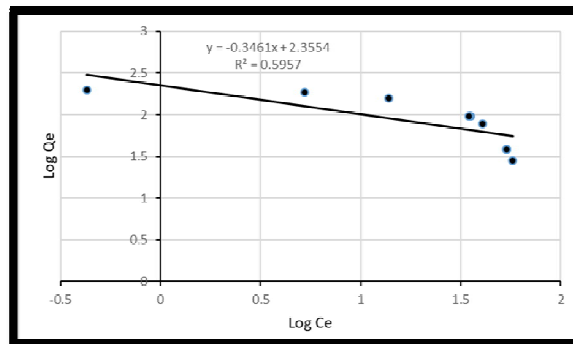


Figure 14: Freundlich Isotherm of D1-D9

Key 4: D1----- 60% acetic acid activated carbon at 400^oc for 20 minutes
 D2-----60% acetic acid activated carbon at 400^oc for 40 minutes
 D3-----60% acetic acid activated carbon at 400^oc for 60 minutes
 D4-----60% acetic acid activated carbon at 500^oc for 20 minutes
 D5-----60% acetic acid activated carbon at 500^oc for 40 minutes
 D6-----60% acetic acid activated carbon at 500^oc for 60 minutes
 D7-----60% acetic acid activated carbon at 600^oc for 20 minutes
 D8-----60% acetic acid activated carbon at 600^oc for 40 minutes
 D9-----60% acetic acid activated carbon at 600^oc for 60 minutes

3.10.2. Dubinin-Radushkevich Isotherm

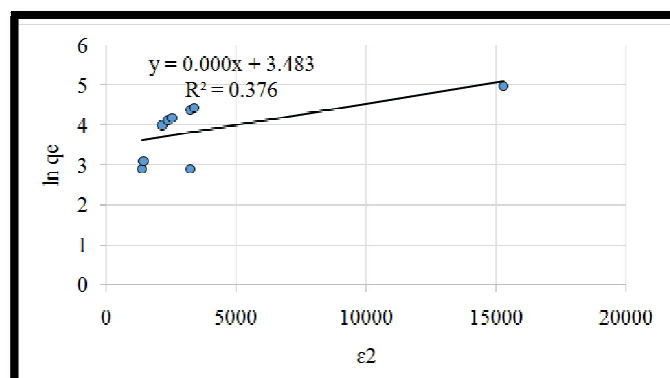


Figure 15: Dubinin-Radushkevich Isotherm of A1-A9

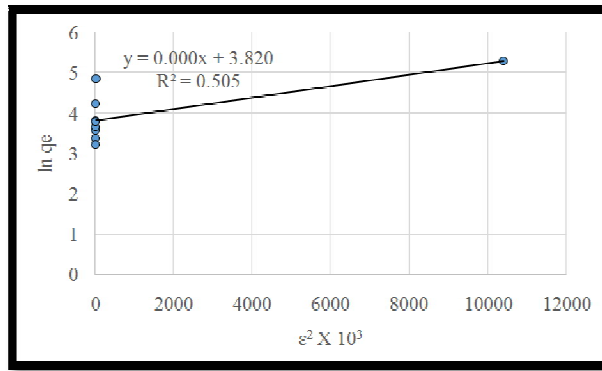


Figure 16: Dubinin-Radushkevich Isotherm of B1-B9

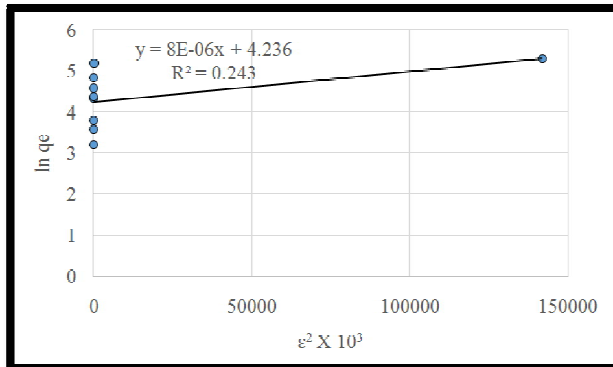


Figure 17: Dubinin-Radushkevich Isotherm of C1-C9

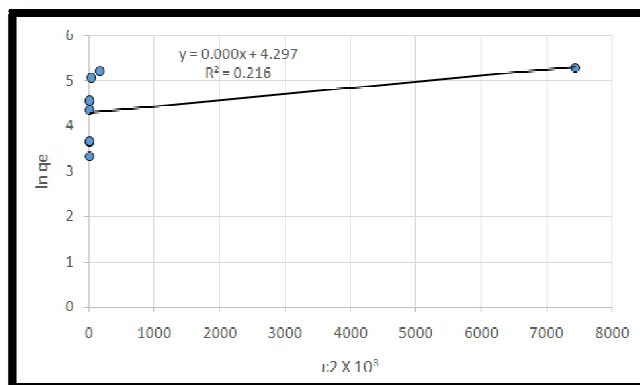


Figure 18: Dubinin-Radushkevich Isotherm of D1-D9

3.10.3. Langmuir Isotherm

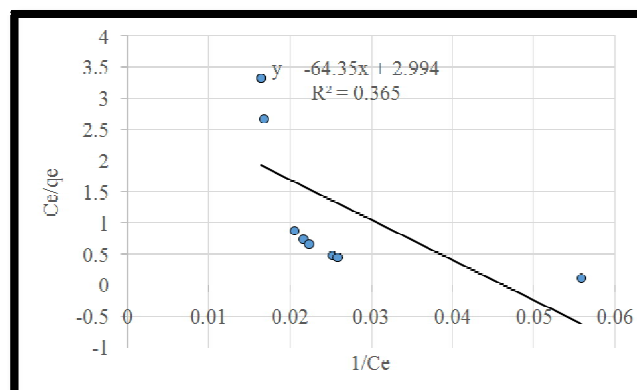


Figure 19: Langmuir Isotherm of A1-A9

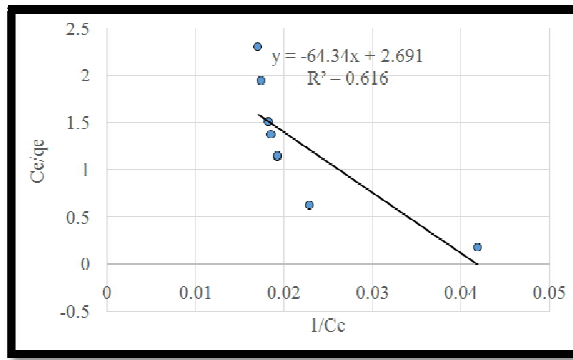


Figure 20: Langmuir Isotherm of B1-B9

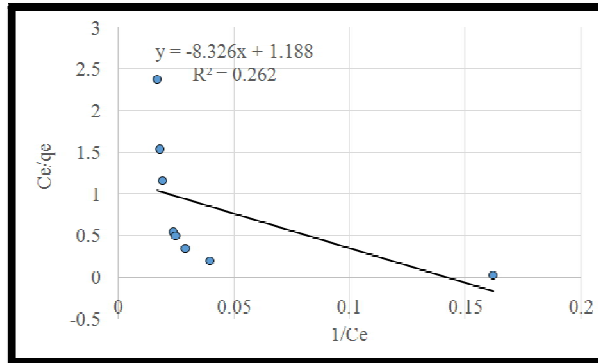


Figure 21: Langmuir Isotherm of C1-C9

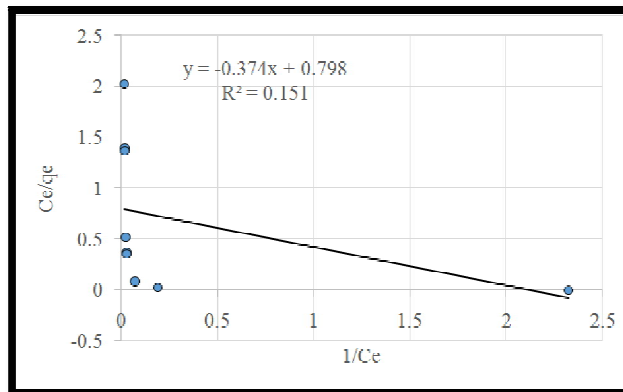


Figure 22: Langmuir Isotherm of D1-D9

3.11. X-Ray Diffraction Patterns

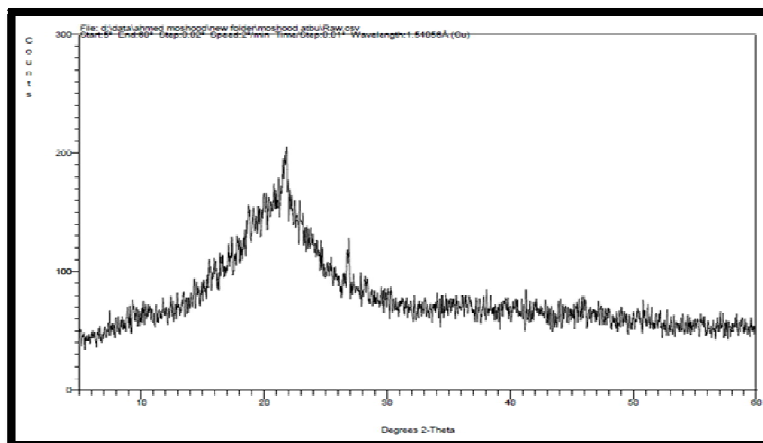


Figure 23: X-Ray Diffraction of Raw Canarium Schwienfurthii

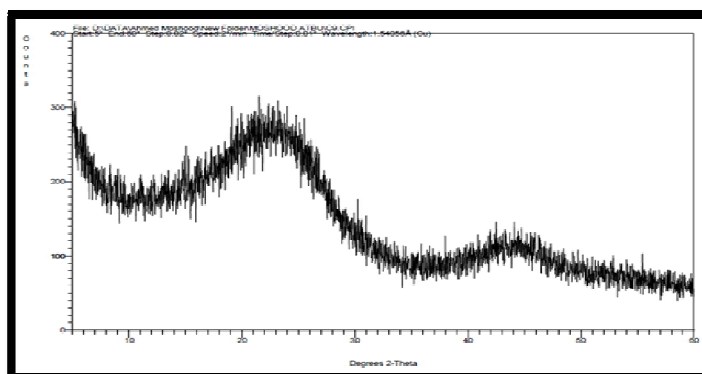


Figure 24: X-Ray Diffraction of Activated Carbon C9

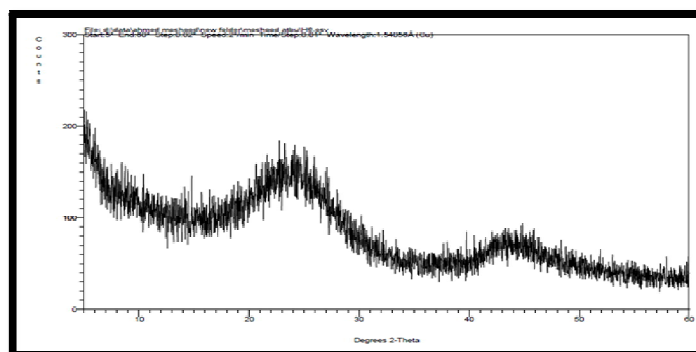


Figure 25: X-Ray Diffraction of Activated Carbon H6

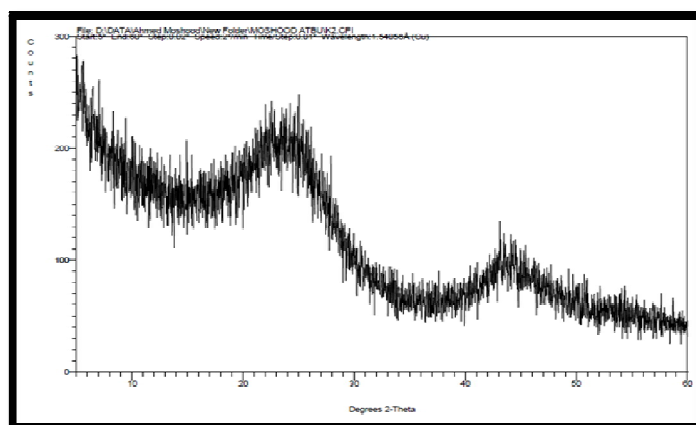


Figure 26: X-Ray Diffraction of Activated Carbon K2

The figure 23 shows the diffraction pattern of the canarium schweinfurthii biomass. It is characterized by diffused halo that appear at 2θ values between 13.0 to 22.0 degrees. There are no significant crystalline peaks, thus confirms the amorphous nature of the material.

However, figure 24 (C9) showed the XRD spectrum of the activated carbon formed by the acetic acid activation at 600 °C for 60 minutes. This figure shows characteristic peak at angles of $2\theta = 24^\circ$ and 45.2° . This peak indicates carbon and graphite structures formation with hkl plane of (002) and (100). The spectrum shows the activated carbon is majorly amorphous and similar result had been reported for activated carbon produced from lignocellulosic raw material [17].

4. Conclusion

The research work showed great result as all optimized activated carbon samples showed great characteristics as observed in literatures of other researchers. The SEM of all samples at different magnifications showed presence of pores. The BET of the samples showed average range of 672 – 1098 m²/g. These surface areas made these activated carbons good candidate for adsorption. The FTIR analysis was also used to determine the presence of functional groups and presence of common functional groups like O-H, C-O, C-H, C-C, C=O were observed.

Lastly the adsorption isotherms analysis showed that the adsorption of dye effluent onto the prepared activated carbons fitted more into Freundlich and Langmuir Isotherm and less into D-R isotherm

5. References

- i. Harry M., and Francisco Rodriguez-Reinoso F. (2006). **Textbook of Activated Carbon**. New York, Elsevier Science and Technology Books. (1): 9-22
- ii. El-Sayed G. O., Yehia M. M., and Asaad A. A. (2014). Assessment of activated carbon Prepared from corncob by chemical activation with phosphoric acid. *Journal of Water Resources and Industry*, **7** (8): 66–75
- iii. Rafie, R. M. (2013). Waste lubricating oil treatment by extraction and adsorption. *International Refereed Journal of Engineering and Science*. (2): 1-11
- iv. Sumrit M., Phansiri M., Wanwimon P., and Sataporn Khumpai (2015). *The Scientific World Journal*. 2015: 1-9.
- v. Freundlich, H. K. (1909). *Academische Bibliothek: Leipzig*
- vi. Saad, S. M., Awwad N. S. and Aboterika H. A. (2008). *The Journal of Hazardous Material*. 154: 992– 997.
- vii. Wood, G. O. (1992). Activated carbon adsorption capacities for vapour. *Journal of Carbon*, 30 (4): 593-599.
- viii. Dubinin, M. M. (1975). 'Physical adsorption of gases and vapours in micropores', *Progress in Surface and Membrane science*. Cadenhead D. A, Danielli J. F. and Rosenberg M. D. [Eds]. 9: 1-70. New York, Academic Press
- ix. Ismaila O. A., Folahan A. A. and Gabriel A. O. (2016). Adsorption of p-Phenylenediamine onto activated carbon prepared from *Jatropha curcas* and *Terminalia catappa* seed coats. *Jordan journal of chemistry*. 11 (1): 50 - 67
- x. Ekebafé L.O., Imanaha J.E., and Okieimen F.E. (2017). Effect of carbonization on the processing characteristics of rubber seed shell. *Arabian journal of chemistry*. 10: S174 - S178
- xi. Harry B. (2019). Food and agricultural organization of the United Nations. Manual on making charcoal 'The quality of charcoal'. Retrieved on June 18, 2019 from <http://www.fao.org/3/x5328e/x5328e0b.htm>.
- xii. Eric M., Isaac O., and Askwar H. (2014). Preparation of activated carbon with desired properties through optimization of impregnating agent. *Research Journal in Engineering and Applied Sciences* **3** (5): 327-331
- xiii. Solum M.S., Pugmire R.J., Jagtoyen M. and Derbyshire F. (1995). Evolution of carbon structure in chemically activated wood. *Journal of Carbon*. **33**: 1247-1254
- xiv. Bacher A. (2002). Infrared spectroscopy handout. Retrieved on January 10, 2020 from www.chem.ucla.edu/~bacher/spectroscopy/IR1.html
- xv. Attia A. A., Girgis B. S. and Fathy N. A. (2008). Dyes Pigments. *Journal of Chemical Engineering Science*. **76** (1): 282–289
- xvi. Hassan, M. A. and Ashfaq, A. (2011). International Conference on Chemical, Biological and Environmental Engineering.
- xvii. Abdulkhalil H. P. S., Jawaid M., Firoozian P., Rashid U., Islam A., and Akil5 H. M. 2013. Activated Carbon from Various Agricultural Wastes by Chemical Activation with KOH: Preparation and Characterization. *Journal of Biobased Materials and Bioenergy* **7**: 1–7